

Machine Learning Derived Graded Lattice Structures

J. Wang* and A. Panesar*

* Department of Aeronautics, Imperial College London, SW7 2AZ, UK

Abstract

Herein, we propose a new lattice generation strategy that is computationally cheaper and produces high-quality geometric definition based on Machine Learning (ML) when compared to traditional methods. To achieve the design of high-performance unit cells, firstly, the optimal mechanical property for each cell region is derived according to the loading condition and the reference density obtained utilising a conventional topology optimisation result. Next, a Neural Network (NN) is employed as an inverse generator which is responsible for predicting the cell pattern for the optimal mechanical property. Training data (~ 500) were collected from Finite Element (FE) analysis with varied cell parameters and then fed to the NN. With the help of ML, the time spent in building the inverse generator is significantly reduced. Furthermore, the ML-based inverse generator can handle different cell types rather than one specific type which facilitates the diversity and optimality of lattices.

Introduction

Lattice structure, as a non-stochastic category of cellular materials[1], has been an attractive topic in structural design due to its ease of geometric control and ability to achieve a high strength-to-weight ratio[2], high robustness, and multi-functions[3][4]. Lattice structure has been employed for the realisation of various functions, like energy absorption[5], heat exchange, thermal insulation, sound attenuation, and vibration isolation, and applied to various applications, especially Aerospace[6], where weight reduction is essential.

The development of Additive Manufacturing (AM) has provided manufacturing process with large flexibility that has facilitated the complex design of lattice structures to be fabricated[7]. different AM processes[8][9] might be chosen for lattice fabrication. Although AM processes extend the design domain to nearly any shape and geometry. But support structure[10], powder removal[11], and other AM-related constraints still needs consideration during the structural design.

To make full use of the extended design space offered by AM, the establishment of lattice generation strategies for design optimisation of lattice structures is essential. The development of this field has produced various lattice design methods. For example, the ground truss structure method[12] is one of the earliest design methods for truss structures, where the geometry and topology of trusses can be formulated as a standard sizing problem. Topology Optimisation (TO) is also a powerful tool applicable to lattice structural design. Several approaches utilised the density distribution from TO result to map the lattices[13][14]. Multi-scale TO[15][16], where the macro and micro scales are optimised simultaneously during the structural optimisation process, is capable of generating high-performance structures with optimised micro lattices.

To further improve the performance of the designed lattice structures and accelerate the design process, Machine Learning (ML) has been applied to lattice design in several attempts. For example, the use of clustering[17] algorithm helps to cluster the elements into different cell clusters. The employment of Neural Network (NN) accelerates the property prediction of lattice unit cells[18], [19], enables the inverse design of spinoid metamaterial[20], and even helps with the sensitivity analysis of TO[21].

In this work, the 2D lattice unit cell is parameterised by the nodal parameters (4 parameters), and its mechanical properties are represented using the elasticity compliance matrix (6 independent components). a Neural Network (NN) is employed as an inverse generator which can output the representative parameters of lattice unit cells with the input elasticity properties. A training dataset with a size of 500 is collected from FE analysis of voxelised cells with varied cell parameters and then fed to the NN. To implement the lattice

generation strategy, firstly, optimal density distribution is obtained from TO result as the reference elemental densities. Secondly, the optimal elasticity properties are determined based on the reference elemental density and the elemental stress condition. Finally, the NN-based inverse lattice generator is used to generate corresponding lattice unit cells from the optimal elasticity properties. A workflow illustrating the whole work is shown as Figure 1.

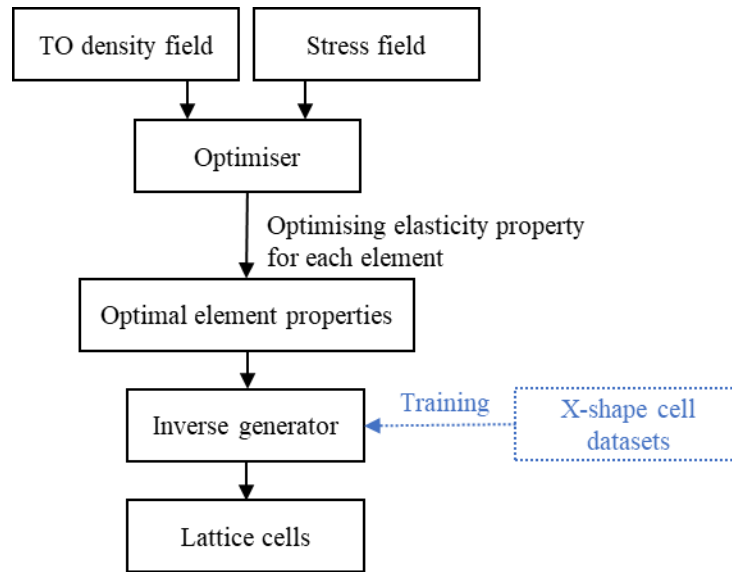


Figure 1: Illustration of the work

The outline of the paper is as follows. First, the main methodology of the proposed strategy is explained, including details on the training of the inverse lattice generator and how the lattice generation strategy operates. Subsequently, an example of the MBB-beam is introduced and the results are discussions about the influences of key factors are provided.

Methodology

Building Inverse Lattice Generator

This work focuses on 2D lattice structures composed of the X-shape lattice cell with a resolution of 15×15 pixels. A cell resolution of 15×15 can provide the lowest cell volume fraction (represented using symbol vf) of 0.129 for the X-shaped cell (see Figure 2). The lowest possible cell volume fraction is sufficient to capture the low-density features in the TO grey structural design.

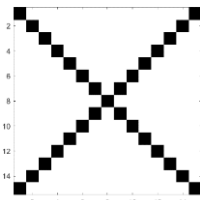


Figure 2: lowest cell vf for different cell types X-shape cell with $vf = 0.129$

The cell representation method adopted in this study is the nodal parameter (see Figure 3). For X-shape cells, 4 nodal parameters are sufficient to represent an X-shape cell exactly.

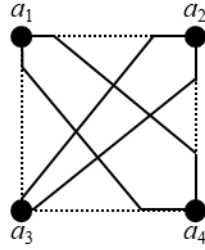


Figure 3: Illustration of nodal parameters for X-shape cell

The elasticity property of the lattice cell is an important factor considered in a compliance minimisation problem. The elasticity compliance matrix \mathbf{Z} is adopted here to represent the lattice cell's anisotropic elasticity property. The elasticity compliance matrix \mathbf{Z} is defined as:

$$\boldsymbol{\varepsilon} = \mathbf{Z}\boldsymbol{\sigma}$$

$$\begin{bmatrix} \varepsilon_1 \\ \varepsilon_2 \\ \varepsilon_3 \end{bmatrix} = \begin{bmatrix} Z_{11} & Z_{12} & Z_{13} \\ Z_{21} & Z_{22} & Z_{23} \\ Z_{31} & Z_{32} & Z_{33} \end{bmatrix} \begin{bmatrix} \sigma_1 \\ \sigma_2 \\ \sigma_3 \end{bmatrix} \quad (1)$$

where $\boldsymbol{\varepsilon}$ is the strain, $\boldsymbol{\sigma}$ is the stress.

For 2D anisotropic material, because of the symmetry of the \mathbf{Z} matrix, there are 6 independent variables in \mathbf{Z} . These 6 independent variables are represented using $z_{11}, z_{12}, z_{13}, z_{22}, z_{23}, z_{33}$ in this paper, where z_{ij} refers to the component in the i -th row and j -th column.

To calculate the six independent components of the elasticity compliance matrix \mathbf{Z} , 2D Finite Element (FE) method is adopted. For each lattice unit cell, the cell pattern is mapped 6×6 times, which means 6 times in x-direction and 6 times in y-direction (see Figure 4). Uni-axial loads and pure shear load are applied to the tessellated lattice cells respectively.

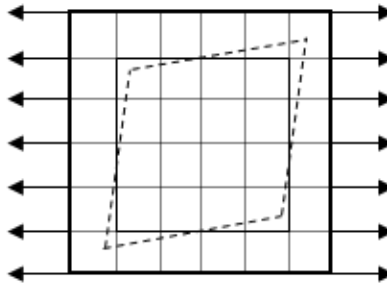


Figure 4: Illustration of the tessellation of lattice unit cells for FE analysis

500 sample X-shape cells are generated randomly with integer nodal parameters and FE analysis is run for each sample cell with the Poisson's ratio of the material to be 0.3. Instead of the elasticity compliance \mathbf{Z} , the elasticity tensor \mathbf{C} is adopted here to show the relationship between cell strength and cell density. The elasticity tensor \mathbf{C} is defined as:

$$\boldsymbol{\sigma} = \mathbf{C}\boldsymbol{\varepsilon} \quad (2)$$

From the elasticity properties collected for the sample X-shape, a series of $C_{ij} - vf$ curves are plotted in Figure 5. The power-law curves with different penalty exponents (the power of vf) are also plotted in Figure 4 as references.

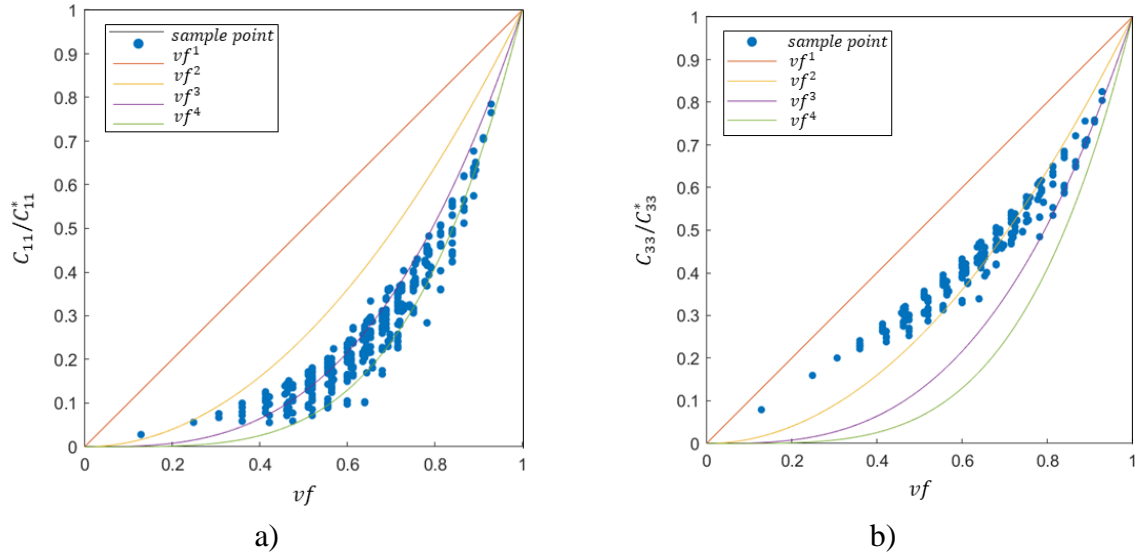


Figure 5: Elasticity tensors vs cell vf (X-shape cell) (a) for C_{11} (b) for C_{33}

From the figure above, it can be concluded that: a) The grading of lattice unit cell enables the diversity of anisotropic properties under the same cell vf . b) The X-shape cell tends to have a higher value of C_{33} but performs worse when resisting normal stress.

The training data size is 500 for X-shape cells as mentioned above. To capture the nonlinearity of the mechanical model, NN is adopted here for a fast and accurate unit cell output. The NN structure in this paper consists of 1 input layer, 3 hidden layers, and 1 output layer. The dimension of input is 6 (the 6 independent components for \mathbf{Z}), while the dimension of output is 4 (the 4 nodal parameters for cell representation).

To evaluate the performance of the trained inverse generator, the accuracy of the trained inverse generator is checked by comparing the reconstructed lattice cell with the corresponding original lattice cell. Figure 6 shows some of the reconstructed lattice cells and their corresponding original cells. In most cases, the inverse generator is able to generate exactly the same cells as the original ones. Only a few cases show slight differences.

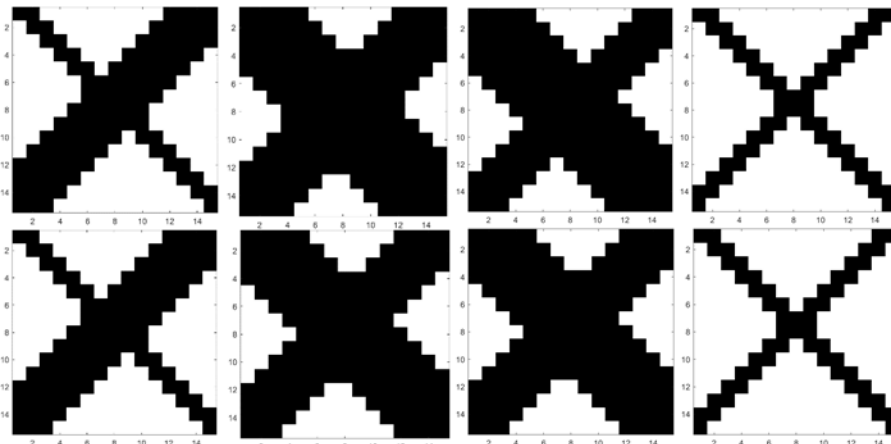


Figure 6: the reconstructed cells and the corresponding original cells

Lattice Generation Strategy

The overall main objective function of the lattice structural optimisation problem is to minimise structural compliance (a measure of the inverse of stiffness). Structural compliance is defined as:

$$\mathbf{Cp} = \frac{1}{2} \mathbf{U}^T \mathbf{K} \mathbf{U} \quad (3)$$

where \mathbf{Cp} is the compliance, \mathbf{K} is the global stiffness matrix and \mathbf{U} is the global displacement vector.

Solid Isotropic Material Penalisation (SIMP)[22] method is a density-based TO approach, which optimises the structure through optimising the densities of the element within the design domain. In this paper, the result from a low-resolution SIMP is utilised as the start point of the proposed lattice generation strategy. Every element in the low-resolution structure will be mapped by a lattice cell and those lattice cells will form a new high-resolution structure.

The overall objective function, which is the structural compliance, also equals the total structural strain energy. To divide the overall optimisation problem into subproblems, the overall structural strain energy is divided into elemental strain energies:

$$\mathbf{SE}_{total} = \sum_{element} \mathbf{SE}_e \quad (4)$$

where \mathbf{SE}_{total} is the total structural strain energy, and \mathbf{SE}_e is the elemental strain energy.

Hence, the sub-problem can be defined as the following equation for the i -th cell region:

$$\begin{aligned} & \min_{\mathbf{Z}_i} \mathbf{SE}_e \\ & \text{subject to: } \mathbf{vf}_i \leq \rho_i(\mathbf{SIMP}) + \varepsilon \end{aligned} \quad (5)$$

where the objective function is set as the elemental strain energy, subject to a volume fraction control. The optimisation variables are the elasticity compliance matrix of the i -th cell region (\mathbf{Z}_i). Cell volume fraction \mathbf{vf}_i is constraint by the relative density ρ_i from SIMP, allowing slight differences between these two values.

Through a series of sub-problems, the anisotropic properties for each element can be optimised. Based on the optimised anisotropic elasticity properties, lattice cells will be predicted through the developed inverse generator. To conclude, the lattice generation strategy consists of three steps (shown in Figure 7): i) produce the greyscale structure using SIMP; ii) generate anisotropic properties for each cell region based on the greyscale SIMP result; iii) use the inverse lattice generator to output lattice unit cells from the anisotropic properties and form the final lattice structure.

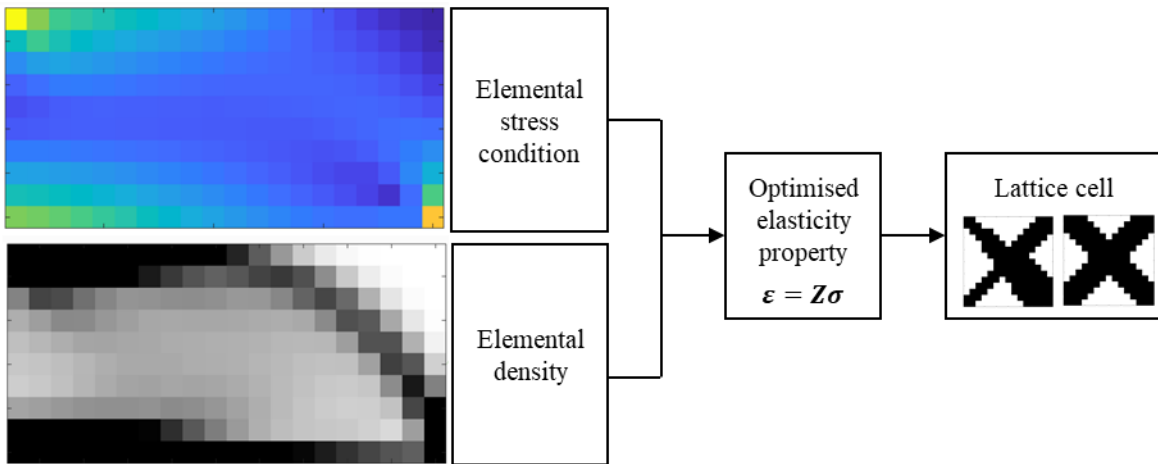


Figure 7: Illustration of the proposed lattice generation strategy

Results and Discussions

Most studies concerning structural optimisation methods consider the classic MBB-beam (in 2D) and therefore this work also utilised such a structure (see Figure 8). To define the design domains, the low-resolution greyscale TO structure consisted of 20×10 elements, while the high-resolution final lattice structure consisted of 300×150 voxels.

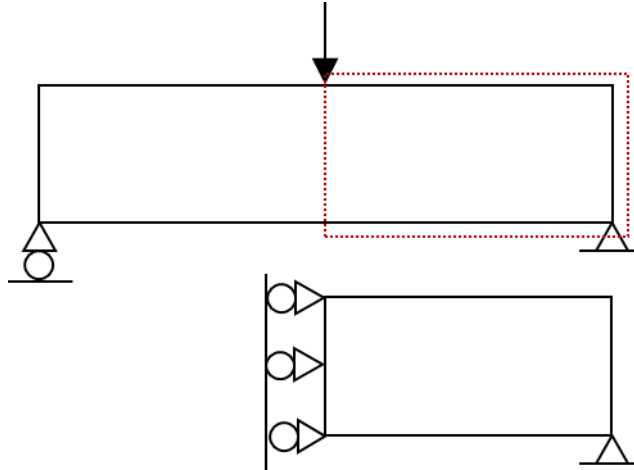


Figure 8: The MBB-beam problem

Total Strain Energy (SE_{total}), which is the objective function of the overall optimisation problem, was set as the performance measure. A lower value of SE_{total} means a stiffer structure. FE analysis was adopted to calculate the values of SE_{total} for the structures.

A greyscale structure of size 20×10 with a total volume fraction (vf) of 0.5 was generated using SIMP with a penalty exponent selected as $p = 3$ as the start point of the proposed lattice generation strategy (see Figure 9).

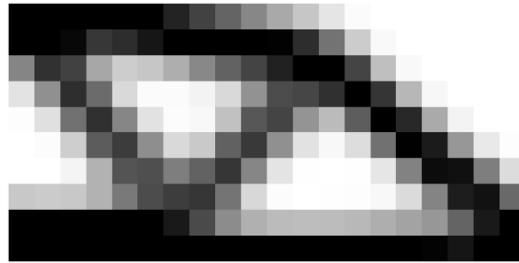


Figure 9: Greyscale SIMP result

Then the anisotropic properties of the 20×10 cell regions were optimised and used to map lattice unit cells through the inverse lattice generator. Figure 10 shows the final lattice structures produced from this new strategy.

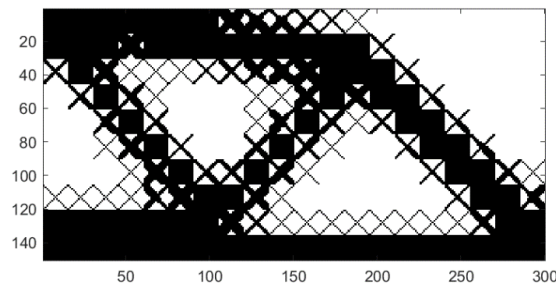


Figure 10: Lattice structure generated by the new strategy

FE analysis with a fine mesh (300×15) was adopted to calculate the value of SE_{total} for the generated lattice structures:

$$SE_{total} = 94.47$$

A benchmark from SIMP with penalisation of 3 gives a clear black and white structure with $SE_{total} = 80$. But the computational time would be 10 times longer than this ML-based strategy.

Conclusion

Lattice structures, which have the instinct of lightweight[23] and robustness, can contribute to the improvement of structural performance. Developments of lattice generation strategies are quite important for achieving the target functions and the acceleration of structural optimisation time. In this work, a novel lattice generation strategy with low time consumption and high-performance output is proposed with the assistance of Machine Learning (ML). The main assistance from ML would be the modelling of the relationship between lattice topologies and lattice properties. An inverse generator which output lattice unit cell with the input target elasticity property is trained based on NN. The proposed strategy starts from density distributions of TO results, then search for the optimal elasticity property for each element, and finally map the elements with lattice cells output from the inverse generator. The presented example lattice structures demonstrate the promising of the proposed lattice generation strategy in generating lattice structures efficiently. Although the compliance increases slightly compared with black and white SIMP result, this strategy is able to give a satisfactory high-resolution design 10 times faster.

Traditional lattice generation strategies are usually based only on density distributions, without considering grading within lattice unit cell. The new method proposed in this work considers anisotropic lattice cells together with uniform lattice cells, which can lead to better utilisation of materials.

The presented lattice generation strategy can be extended in several ways: (a) developing post-processing method to trim extra useless trusses. (b) involving multiple cell types; (c) applying to 3D lattice structures.

Reference

- [1] W. Tao and M. C. Leu, "Design of lattice structure for additive manufacturing," 2016. doi: 10.1109/ISFA.2016.7790182.
- [2] T. Maconachie *et al.*, "SLM lattice structures: Properties, performance, applications and challenges," *Materials and Design*, vol. 183. 2019. doi: 10.1016/j.matdes.2019.108137.
- [3] C. Lee, E. S. Greenhalgh, M. S. P. Shaffer, and A. Panesar, "Optimized microstructures for multifunctional structural electrolytes," *Multifunctional Materials*, vol. 2, no. 4, 2019, doi: 10.1088/2399-7532/ab47ed.
- [4] H. N. G. Wadley, "Multifunctional periodic cellular metals," *Philosophical Transactions of the Royal Society A: Mathematical, Physical and Engineering Sciences*, vol. 364, no. 1838, 2006, doi: 10.1098/rsta.2005.1697.
- [5] J. Plocher and A. Panesar, "Effect of density and unit cell size grading on the stiffness and energy absorption of short fibre-reinforced functionally graded lattice structures," *Additive Manufacturing*, vol. 33, 2020, doi: 10.1016/j.addma.2020.101171.
- [6] E. del Olmo *et al.*, "Lattice structures for aerospace applications," in *European Space Agency, (Special Publication) ESA SP*, 2012, vol. 691 SP.
- [7] J. Plocher and A. Panesar, "Review on design and structural optimisation in additive manufacturing: Towards next-generation lightweight structures," *Materials and Design*, vol. 183. 2019. doi: 10.1016/j.matdes.2019.108164.

- [8] L. E Murr, S. M Gaytan, and E. Martinez, "Fabricating Functional Ti-Alloy Biomedical Implants by Additive Manufacturing Using Electron Beam Melting," *Journal of Biotechnology & Biomaterials*, vol. 02, no. 03, 2012, doi: 10.4172/2155-952x.1000131.
- [9] K. C. R. Kolan, M. C. Leu, G. E. Hilmas, and T. Comte, "Effect of architecture and porosity on mechanical properties of borate glass scaffolds made by selective laser sintering," 2013.
- [10] J. Jiang, X. Xu, and J. Stringer, "Support Structures for Additive Manufacturing: A Review," *Journal of Manufacturing and Materials Processing*, vol. 2, no. 4, 2018, doi: 10.3390/jmmp2040064.
- [11] W. Ameen, A. Al-ahmari, and H. Alkhalefah, "Design the support structures for easy removal of unmelted powder in metal additive manufacturing," *International Journal of Advanced Manufacturing Technology*, vol. 29, no. 02, 2020.
- [12] M. P. Bendsøe, A. Ben-Tal, and J. Zowe, "Optimization methods for truss geometry and topology design," *Structural Optimization*, vol. 7, no. 3. 1994. doi: 10.1007/BF01742459.
- [13] A. Panesar, M. Abdi, D. Hickman, and I. Ashcroft, "Strategies for functionally graded lattice structures derived using topology optimisation for Additive Manufacturing," *Additive Manufacturing*, vol. 19, 2018, doi: 10.1016/j.addma.2017.11.008.
- [14] D. Brackett, I. Ashcroft, and R. Hague, "Topology optimization for additive manufacturing," 2011.
- [15] J. Wu, O. Sigmund, and J. P. Groen, "Topology optimization of multi-scale structures: a review," *Structural and Multidisciplinary Optimization*, vol. 63, no. 3. 2021. doi: 10.1007/s00158-021-02881-8.
- [16] Y. Wang, F. Chen, and M. Y. Wang, "Concurrent design with connectable graded microstructures," *Computer Methods in Applied Mechanics and Engineering*, vol. 317, 2017, doi: 10.1016/j.cma.2016.12.007.
- [17] K. Liu, A. Tovar, E. Nutwell, and D. Detwiler, "Towards nonlinear multimaterial topology optimization using unsupervised machine learning and metamodel-based optimization," in *Proceedings of the ASME Design Engineering Technical Conference*, 2015, vol. 2B-2015. doi: 10.1115/DETC201546534.
- [18] R. Kulagin, Y. Beygelzimer, Y. Estrin, A. Schumilin, and P. Gumbsch, "Architected Lattice Materials with Tunable Anisotropy: Design and Analysis of the Material Property Space with the Aid of Machine Learning," *Advanced Engineering Materials*, vol. 22, no. 12, 2020, doi: 10.1002/adem.202001069.
- [19] N. Després, E. Cyr, P. Setoodeh, and M. Mohammadi, "Deep Learning and Design for Additive Manufacturing: A Framework for Microlattice Architecture," *JOM*, vol. 72, no. 6, 2020, doi: 10.1007/s11837-020-04131-6.
- [20] S. Kumar, S. Tan, L. Zheng, and D. M. Kochmann, "Inverse-designed spinodoid metamaterials," *npj Computational Materials*, vol. 6, no. 1, 2020, doi: 10.1038/s41524-020-0341-6.
- [21] D. A. White, W. J. Arrighi, J. Kudo, and S. E. Watts, "Multiscale topology optimization using neural network surrogate models," *Computer Methods in Applied Mechanics and Engineering*, vol. 346, 2019, doi: 10.1016/j.cma.2018.09.007.
- [22] O. Sigmund and K. Maute, "Topology optimization approaches: A comparative review," *Structural and Multidisciplinary Optimization*, vol. 48, no. 6. 2013. doi: 10.1007/s00158-013-0978-6.
- [23] M. Królikowski and D. Grzesiak, "Technological Restrictions of Lightweight Lattice Structures Manufactured by Selective Laser Melting of Metals," *Advances in Manufacturing Science and Technology*, vol. 38, no. 2, 2014, doi: 10.2478/amst-2014-0012.